nature genetics

Age-related macular degeneration is associated with an unstable *ARMS2* (*LOC387715*) mRNA

Lars G Fritsche[1,4], Thomas Loenhardt[1,4], Andreas Janssen[1], Sheila A Fisher[2], Andrea Rivera[1], Claudia N Keilhauer[3] & Bernhard H F Weber[1]

Age-related macular degeneration (AMD) is a prevalent multifactorial disorder of the central retina[1–3]. Genetic variants at two chromosomal loci, 1q31 and 10q26, confer major disease risks, together accounting for more than 50% of AMD pathology[4–9]. Signals at 10q26 center over two nearby genes, *ARMS2* (age-related maculopathy susceptibility 2, also known as *LOC387715*)[8,9] and *HTRA1* (high-temperature requirement factor A1)[10,11], suggesting two equally probable candidates. Here we show that a deletion-insertion polymorphism in *ARMS2* (NM_001099667.1:c.* 372_815del443ins54) is strongly associated with AMD, directly affecting the transcript by removing the polyadenylation signal and inserting a 54-bp element known to mediate rapid mRNA turnover. As a consequence, expression of *ARMS2* in homozygous carriers of the indel variant is not detectable. Confirming previous findings[12], we demonstrate a mitochondrial association of the normal protein and further define its retinal localization to the ellipsoid region of the photoreceptors. Our data suggest that *ARMS2* has a key role in AMD, possibly through mitochondria-related pathways.

On the basis of its putative role in extracellular matrix homeostasis[13], *HTRA1* seems an obvious functional candidate within the AMD-associated locus at 10q26 (refs. 8,9). Nevertheless, reports of a causal variant in the promoter region of *HTRA1* (refs. 10,11) could not be verified either by us (data not shown) or by others[12]. In contrast, *ARMS2* is an evolutionarily recent gene within the primate lineage and, so far, no biological properties have been attributed to the putative protein. There is strong linkage disequilibrium (LD) across the *ARMS2-HTRA1* region, making genetic association studies alone insufficient to distinguish between the two candidates. Instead, a comprehensive characterization of AMD-associated variants in the region of high LD is warranted, closely accompanied by a sophisticated analysis of their possible functional relevance in the disease process.

To first delineate the extent of the AMD-associated risk haplotype within the 10q26 region, we genotyped 28 SNPs uniformly distributed across a 107-kb *ARMS2-HTRA1* interval in 794 individuals with nonfamilial AMD and 612 unrelated controls[9]. All control genotypes were in Hardy-Weinberg equilibrium ($P > 0.1$). Five highly correlated SNPs (rs10490924, rs3750848, rs3793917, rs11200638 and rs932275; $r^2 < 0.88$) showed strongest association with AMD ($2.72 < \mathrm{OR} < 2.86$, $10^{-29} < P < 10^{-27}$; **Table 1**, **Supplementary Fig. 1a,c** and **Supplementary Table 1** online). These SNPs also include the *ARMS2* A69S variant (rs10490924) initially reported to show highest association with AMD[8,9], and the putative functional *HTRA1* promoter variant rs11200638, suggested to influence the binding properties of transcription factor activator protein 2 and serum response factor[10,11]. Haplotype analysis demonstrated that these SNPs reside within a 23.3-kb region of LD extending from 3,168 bp centromeric of *ARMS2* exon 1 (rs2736930) to 12,645 bp telomeric of *HTRA1* exon 1 halfway into intron 1 (rs2672591) (**Supplementary Fig. 1**). The five SNPs tag a single risk haplotype that includes ten SNPs in total (rs2736930, rs10490924, rs3750848, rs2014307, rs3793917, rs11200638, rs2248799, rs932275, rs2736914 and rs2672591; **Supplementary Table 2** online).

To search for additional risk-associated variants, we next resequenced the entire 23.3-kb LD region in 16 unrelated individuals with AMD. To maximize power to detect variants occurring on the single risk haplotype established, we selected cases heterozygous ($N = 6$) and homozygous ($N = 5$) for this risk haplotype, and another five individuals with AMD homozygous or compound heterozygous for any of the four most common nonrisk haplotypes (**Supplementary Table 2**). In total, we detected 54 distinct variants, of which 15 occurred exclusively on the established risk haplotype ($r^2 = 1$) (**Supplementary Table 3** online). One of these 15 variations resides within the 3′-UTR of the *ARMS2* gene and represents a combination of a deletion and insertion (*372_815delins54). The deletion removes the polyadenylation signal sequence at position *395_400 exclusively used for the addition of a poly(A) tract 19 bp downstream (**Fig. 1a** and data not shown). The insertion introduces a 54-bp AU-rich element (**Fig. 1a**), known for its properties to control mRNA decay in many transcripts that encode a wide variety of proteins involved in transient biological processes[14–16]. Of the remaining 14 SNPs, rs10490924 and rs11200638 have been discussed before[8–11], ten SNPs are intronic or intergenic and two are synonymous SNPs in

[1]Institute of Human Genetics, University of Regensburg, Franz-Josef-Strauss-Allee 11, 93053 Regensburg, Germany. [2]Department of Medical and Molecular Genetics, King's College and St Thomas' Hospitals, London, WC2R 2LS, UK. [3]Department of Ophthalmology, University of Wuerzburg, 97080 Wuerzburg, Germany. [4]These authors contributed equally to this work. Correspondence should be addressed to B.H.F.W. (bweb@klinik.uni-regensburg.de).

Received 4 February; accepted 18 April; published online 30 May 2008; doi:10.1038/ng.170

Table 1 Six highly correlated risk alleles ($r^2 > 0.88$) residing on a single risk haplotype within the 23.3-kb LD region at *ARMS2-HTRA1*

Marker	Gene	Role	Risk allele	Minor allele frequency		Association results[a]	
				AMD ($N = 760$)	Control ($N = 549$)	Odds ratio[b] (95% CI)	*P* value
rs10490924	*ARMS2*	Coding (A69S)	T	0.424	0.193	2.86 (2.38–3.44)	2.8×10^{-29}
rs3750848	*ARMS2*	Intronic	G	0.424	0.193	2.86 (2.38–3.44)	2.8×10^{-29}
del443ins54	*ARMS2*	3′ UTR	del443ins54	0.424	0.193	2.85 (2.37–3.43)	4.1×10^{-29}
rs3793917	–	Intergenic	G	0.426	0.201	2.72 (2.27–3.26)	1.5×10^{-27}
rs11200638	*HTRA1*	Promoter	A	0.426	0.199	2.85 (2.37–3.42)	6.9×10^{-29}
rs932275	*HTRA1*	Intronic	A	0.412	0.191	2.83 (2.35–3.41)	6.1×10^{-28}

[a]Association analyses were done using logistic regression assuming an additive model. [b]Odds ratios are derived from logistic regression parameter estimates for a single copy of the risk allele; homozygous risks can be obtained from the square of the heterozygous risk.

HTRA1 exon 1. Although not formerly excluded for their possible role in AMD pathogenesis, the latter two groups of variants seem rather unlikely to exert consequences on gene function.

The potential functional effects of the *372_815delins54 variant on the stability of the *ARMS2* transcript led us to further test this polymorphism for association in the initial collection of AMD cases and controls. The indel variant showed highly significant association with AMD compared to controls (42.4% vs. 19.3%, $P = 4.1 \times 10^{-29}$). The odds ratios for this variant are similar to those observed for several other SNPs on the risk haplotype with a 2.9-fold increased risk in individuals carrying a single copy of the risk allele compared with an 8.1-fold increased risk in homozygous individuals (**Table 1**).

Next, we compared allelic *ARMS2* mRNA expression in three retinal and six placental samples of unrelated non-AMD individuals, all heterozygous at the genomic level for the indel variant and the tightly associated A69S (rs10490924) polymorphism (**Fig. 1b**). In the samples analyzed, RT-PCR with first-strand cDNAs, either primed with oligo-dT or gene-specific oligonucleotides, revealed exclusively the presence of the Ala69 allele, which is not associated with risk. To determine the sensitivity of allelic discrimination by our sequencing approach, we analyzed dilution series of plasmid clones carrying either the Ala69 or the Ser69 variant of *ARMS2* (**Supplementary Fig. 2** online). Our data demonstrate that the limits of allelic resolution by sequencing range between 1:12 to 1:13, suggesting that in the tissue samples tested, the indel *ARMS2* isoform is reduced over the regular transcript by a ratio of 1:12 or less. To test the stability of the two isoforms, we carried out RNA blot analysis of heterologously expressed *ARMS2* variants. Each isoform was expressed in EBNA 293 cells from its genomic locus comprising 3,749 bp (nonrisk isoform) and 3,360 bp (risk isoform), respectively. Strong transcription initiation (TI) site and polyadenylation signal sequences were provided by the vector construct. RNA was harvested 24 h after transfection and showed a markedly reduced amount of the indel transcript (1.7 kb) compared to the normal variant (2.1 kb) (**Fig. 1c**).

To analyze ARMS2 protein expression, we generated rabbit polyclonal antibodies against the recombinant full-length 107 amino acid peptide[9]. Subsequent epitope mapping with a series of overlapping 15 amino acid peptides demonstrated a high specificity for the VLDPGVG epitope of ARMS2 (**Fig. 2a**). Protein blot analysis of immunoprecipitated ARMS2 protein from various human tissues showed a predicted protein species of approximately 13.5 kDa in placenta and, less pronounced, in retinas of several non-AMD donors (**Fig. 2b**). We observed weak signals in kidney, lung and heart only after overexposure of the autoradiogram (data no shown), suggesting ubiquitous expression, although with variable rates in the respective tissues. Before protein analysis, all tissues were genotyped and shown to carry exclusively *ARMS2* nonrisk haplotypes (data not

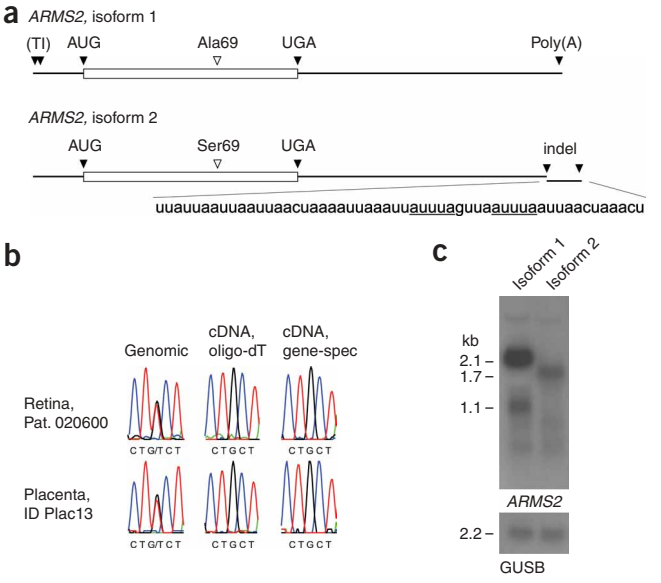

Figure 1 *ARMS2* isoforms and effects of the indel variant on gene expression. (**a**) For isoform 1, transcription initiation (TI) sites at –65 nt and –75 nt and a functional polyadenylation site, AATAAA (poly(A)), were determined by RACE (see Methods). Isoform 2 derives from a deletion-insertion event that adds two conserved AUUUA motifs (underlined) within the 3′-UTR. (**b**) Germline heterozygotes for the A69S variant express a single transcript in retinal or placental tissue corresponding to the nonrisk associated transcript (Ala69). (**c**) RNA blot of heterologously expressed *ARMS2* isoforms. Note the marked difference in signal strength at 2.1 and 1.7 kb. Beta-glucoronidase (GUSB) served as control for RNA integrity and equal mRNA loading.

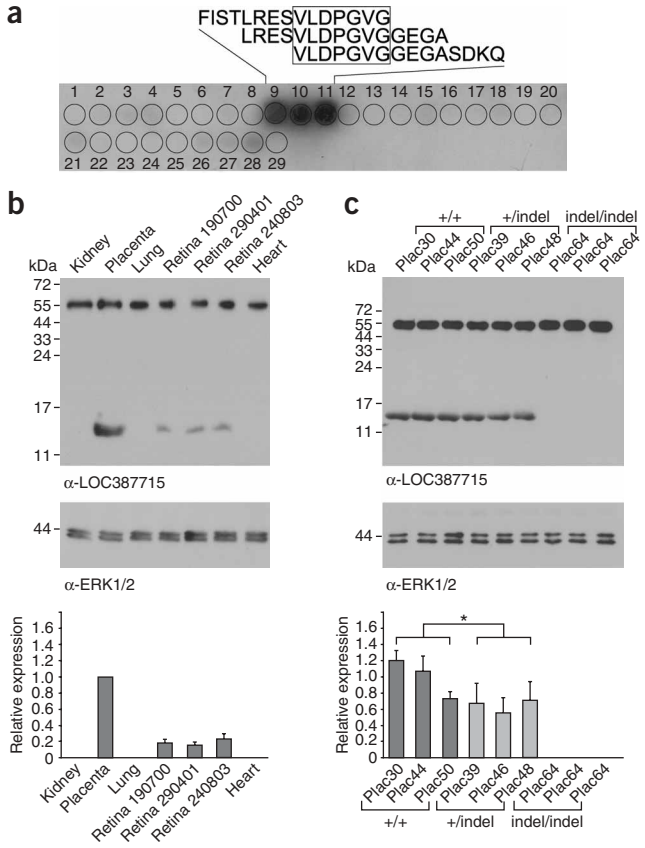

shown). The protein blot signals were consistent with relative expression measurements in previous mRNA expression studies[9,12].

We then assessed protein expression with respect to *ARMS2* genotypes. From a total of 66 randomly collected placentas, we identified 45 samples homozygous or compound heterozygous for one of the nonrisk haplotypes, as well as 20 heterozygous and 1 homozygous carrier for the unique indel risk haplotype. In agreement with RT-PCR data (data not shown), immunoblot analysis showed expression of the 13.5-kDa ARMS2 protein only in placentas from individuals with one or two nonrisk haplotypes. In contrast, three independent preparations from the homozygous carrier of the indel risk haplotype lacked ARMS2 protein expression (**Fig. 2c**).

Finally, immunolocalization of the ARMS2 protein in the human retina showed an intense staining within the photoreceptor layer and a minor dot-like staining in the inner nuclear layer (**Fig. 3a**,**b**). Pre-blocking of the ARMS2 antibody with recombinant full-length protein abolished labeling, further supporting the high specificity of the

Figure 2 Analysis of ARMS2 protein expression. (**a**) Epitope mapping of polyclonal ARMS2 antibody by peptide scanning (**Supplementary Table 5** online). Specific signals correspond to consensus sequence VLDPGVG (boxed). (**b**) Immunoblot analysis of ARMS2 expression in various tissues, including retinas from three unrelated donors. Before analysis, all tissues were genotyped and found to be homozygous for *ARMS2* isoform 1. α-LOC387715, antibody to ARMS2; α-ERK1/2, antibody to ERK1/2. (**c**) Placental ARMS2 protein expression in relation to the *372_815delins54 (indel) genotype. Before immunoprecipitation, supernatants of tissue homogenates were normalized to soluble extracellular signal–regulated kinase 1/2 (ERK1/2). Signals at 50–55 kDa correspond to the immunoglobulin heavy chain. The bottom panels show relative expression representing the mean values of three independent protein blot analyses, respectively. Asterisk indicates a double-sided *P* value of 0.004. Error bars, s.e.m.

antibody staining (**Fig. 3c**). Double-labelings of antibody to ARMS2 with a rod-specific monoclonal antibody (anti-rhodopsin, anti-Rho1D4) (**Fig. 3d**) and the cone-specific peanut agglutinin (PNA) (**Fig. 3e**) indicated an association of ARMS2 with both the rod and cone photoreceptor inner segments. Overlaying immunostainings of ARMS2 and retinoschisin, the latter known to specifically stain the external surfaces of rod and cone photoreceptor inner segments[17], refined the localization of ARMS2 to the mitochondria-enriched ellipsoid region of the inner segments (**Fig. 3f**). This was confirmed with a mitochondrial marker, anti-MTCO2, which fully co-localizes with ARMS2 (**Fig. 3g**). Taken together, immunohistochemical analysis associates ARMS2 with mitochondria most prominently in the ellipsoid region of the rod and cone inner segments (**Fig. 3h**). Adding to previous findings[12] that have shown localization of ARMS2 to the mitochondria in COS-1 transfected cells, we show that endogenous ARMS2 protein is presumably present in mitochondria of other cells as well, although at levels probably below the sensitivity of immunohistochemistry.

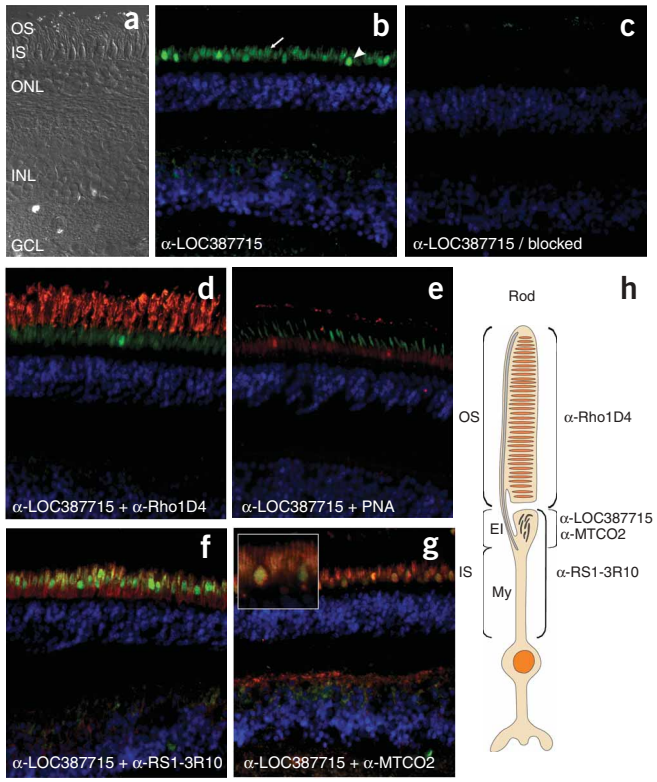

Figure 3 Localization of ARMS2 in the human retina. (**a**) Differential interference contrast image demonstrate retinal layers: OS, outer segment; IS, inner segment; ONL, outer nuclear layer; INL, inner nuclear layer; GCL, ganglion cell layer. (**b**) ARMS2 immunolabeling of a defined IS region in cone (arrowhead) and rod (arrow) photoreceptors. (**c**) Pre-blocking of antibodies with recombinant ARMS2 protein. (**d**) Double labeling of ARMS2 (green) and rod photoreceptor-specific rhodopsin (red). (**e**) Double labeling of ARMS2 (red) and cone photoreceptor-specific peanut-agglutinin (PNA, green). (**f**) Double labeling of ARMS2 (green) and retinoschisin (red). (**g**) Double labeling of ARMS2 (green) and mitochondrial marker MTCO2 (red). (**h**) Schematic summarizing immunolabelings for rod photoreceptors. Counterstaining with DAPI nuclear dye (blue). α-LOC387715, antibody to ARMS2; α-Rho1D4, antibody to rod rhodopsin; α-RS1-3R10, antibody to retinoschisin; α-MTCO2, antibody to mitochondrial epitopes.

On the basis of our and additional data[12], we propose a functional role of ARMS2 in mitochondrial homeostasis, although the precise mode of action remains to be elucidated. In addition to 14 SNPs of unknown functional consequences, we identified a frequent indel polymorphism in the *ARMS2* gene; together, these comprise a single haplotype most strongly associated with AMD. This polymorphism gives rise to an alternative *ARMS2* isoform highly unstable at the mRNA level, consequently resulting in absence of protein expression. These findings strongly suggest that this polymorphism is the sought-after functional variant with relevance to AMD etiology, although formal exclusion of functional consequences for the remaining SNPs on the risk haplotype is ultimately required. The coding SNP rs2736911, which results in a premature stop (R38X) in the ARMS2 protein, is also of interest (**Supplementary Table 3**). As this SNP results in a truncated protein with likely similar consequences for protein function as the indel polymorphism, one would expect similar risks associated with the two variants. SNP rs2736911, however, lies exclusively on a nonrisk haplotype (GGTGCGTGCT; **Supplementary Table 2**). A test of equality of odds ratios showed no difference in the risk associated with this single haplotype compared with the pooled set of all other nonrisk haplotypes ($P = 0.96$). Thus, contrary to our expectations, this variant seems to have a neutral effect.

Mitochondria-associated diseases are increasingly recognized as a diverse group of many clinical entities that develop as a consequence of abnormalities in energy supply, generators of reactive oxygen species and initiators of apoptotic processes[18]. For many years, such mitochondrial functions have frequently been connected to current concepts of AMD pathogenesis[19]. Thus, characterization of the properties of ARMS2 promises new insight into the role of mitochondria in the development of AMD, and may also shed light on general mechanisms of mitochondrial dysfunction in other neurodegenerative disorders of complex etiology[20].

METHODS

Cases and controls. The case-control sample used in the study consisted of 794 individuals with nonfamilial AMD (64.4% females; mean age 76.8 ± 6.6) and 612 unrelated control individuals (62.1% females; mean age 76.2 ± 5.3). All individuals originated from the Lower Franconian area in Bavaria, Southern Germany, and were exclusively recruited at the University Eye Clinic Würzburg between 2001 and 2004. Criteria for inclusion and exclusion of cases and controls have been described elsewhere[9].

The study was approved by the Ethics Committee of the University of Würzburg and adhered to the tenets of the Declaration of Helsinki. All subjects, both cases and controls, were informed about the nature of the study and signed a written consent before blood withdrawal.

Retinal and placental tissue. Human eye bulbs from unrelated donors were obtained over a period of several years from the Human Eye Bank at the University Eye Clinic, Würzburg, Germany. A total of 66 placental tissue samples were received within a 4-month period from St. Hedwig Clinics, Regensburg, Germany. Immediately after receipt, all tissues were placed in liquid nitrogen and stored at –80 °C for further use.

SNP genotyping. We extracted genomic DNA from peripheral blood according to established protocols. We genotyped 28 SNPs with minor allele frequencies ≥ 0.15, equally spaced over a 107-kb region encompassing the 3′-region of *PLEKHA1* and *ARMS2*, and the 5′-region of *HTRA1* (HapMap release 21). SNP genotyping was done as described previously[9]. All SNPs showed high genotyping quality, with an average call rate of 97.4%. Of all genotypings, 3.4% were done in duplicate, resulting in a concordance of ≥99.9%. We did not observe any significant deviations from Hardy-Weinberg equilibrium (HWE) in the controls ($P > 0.1$, **Supplementary Table 1**).

Statistical analysis. We assessed HWE for cases and controls by simulation methods implemented in the Genetics package of R. We carried out single SNP association tests using logistic regression analysis done using R, assuming an additive model on a log scale consistent with the previously described best-fitting genetic model for this locus[9]. We evaluated parameter estimates by applying likelihood ratio tests. Odds ratios and 95% confidence intervals for each copy of the risk allele compared with the nonrisk wild-type genotype were obtained directly from logistic regression parameter estimates. Haplotype blocks were defined using the algorithm of Gabriel *et al.* 2002 implemented in Haploview 4.0 (refs. 21,22). We calculated haplotype frequencies and haplotype-specific odds ratios with UNPHASED[23,24], pooling all rare haplotypes with an estimated frequency <1%. Only fully genotyped individuals were included in SNP and haplotype analysis (**Supplementary Tables 1** and **2**).

Resequencing. We sequenced overlapping PCR fragments covering chr10:124,201,002–124,224,274 (hg18 assembly; **Supplementary Fig. 1**) in 16 individuals with AMD. Regions chr10:124,201,002–124,203,962 and chr10:124,221,869–124,222,467 were not analyzed because of extensive repeat structures. Sequencing was done as described[25]. All variants identified are given in **Supplementary Table 3**.

Characterization of *ARMS2* isoforms. To determine major transcription initiation (TI) and functional polyadenylation sites, we conducted 5′ and 3′ RACE experiments. RNA from placental tissues homozygous for the Ala69 or the Ser69 genotype was isolated by the RNeasy Mini Kit followed by DNAse I treatment (Qiagen). RNA was reverse transcribed using RevertAid M-MuLV Reverse Transcriptase (Fermentas).

For 5′ RACE, first strand cDNA was generated with gene-specific primer Loc-ex2-R. After C-tailing (200 μM dCTP) and terminal deoxynucleotidyl transferase (Invitrogen), a first PCR amplification with anchor primer 5AAP and primer Loc-ex2-R was followed by a second reaction with nested oligonucleotide primers 5′AUAP and Plekha1-SNP12-R. For 3′-RACE, first strand cDNA was done with the SMART-CDS primer (Clontech). This was followed by a first PCR reaction with primers Loc-ex1-F2 and SMART5′PCR and subsequently a second reaction with nested primers Loc-ex1-F and SMART5′PCR. All primer sequences are given in **Supplementary Table 4** online.

RACE products were ligated into pGEM-T Easy (Promega), and approximately 60 single-positive clones were sequenced. RACE in homozygous Ser69 RNA repeatedly failed to result in specific PCR products.

Expression analysis. Six placentas and three retinas were heterozygous for the ARMS2 A69S variant. Genomic PCR amplification was achieved with primers LOC-ex1-F2 and PLEKHA1-SNP12-R, followed by sequencing with primer LOC-ex1-F. RNA from the nine samples was reverse transcribed with either *ARMS2*-specific primer Loc-3′UTR-R or a poly(dT) primer. To be consistent with the genomic PCR amplification, we carried out RT-PCR reactions and sequencing with primers identical to those described above.

Sensitivity to discriminate heterozygous signals by regular sequencing was determined by a titration approach in which plasmid DNAs carrying either the Ala69 or the Ser69 variant were mixed at defined ratios. To obtain the Ser69 clone variant, we carried out site-directed mutagenesis with clone pGEM-T/10490924G carrying the Ala69 variant. Plasmid DNAs were mixed in the following ratios: 1:1, 1:2, 1:4, 1:8, 1:10, 1:11, 1:12, 1:13, 1:14, 1:16 and 1:32. These mixes were PCR amplified with primers LOC-ex1-F and PLEKHA1-SNP12-R and subsequently sequenced with forward primer LOC-ex1-F (**Supplementary Fig. 2**).

For heterologous RNA expression in EBNA 293 cells, genomic loci of *ARMS2* isoform 1 and 2 were PCR amplified from placental tissues homozygous for Ala69 or Ser69, respectively. We used Loc-5′UTR-F and PRSS11-SNP5-R2 primers. Each PCR product (3,749 bp and 3,360 bp, respectively) was cloned into expression vector pCEP4 (Invitrogen).

EBNA 293 cells were transfected with Fugene HD (Hoffmann-La Roche) and plasmid DNA (2 μg). Co-transfection with green fluorescent protein in pCEP4 served as control for transfection efficiency, which was consistently >50%. After 24 h, total RNA was extracted and 10 μg electrophoretically separated in a 1% formaldehyde gel. After blotting, the membrane was hybridized with a ^{32}P-dCTP (6.000 Ci/mmol) labeled probe generated with primers Loc-ex1-F2

and Loc-ex2-R. A 455-bp β-glucoronidase (GUSB)-specific probe (PCR product with primers GUSB6 and GUSB7) served as control for RNA integrity and equal loading.

Generation of polyclonal antibodies and epitope mapping. A polyclonal antibody was generated commercially in rabbits immunized with full-length recombinant ARMS2 protein (ImmunoGlobe Antikörpertechnik). Epitope mapping was done by protein blot analysis with overlapping 15meric peptides (5 nmol each), together representing the entire amino acid sequence of ARMS2 (ref. 26).

Protein blot analysis. Samples were denatured in 1× Laemmli buffer (10 mM Tris-HCl, pH 6.8, 4% SDS, 10% glycerol, 4% β-mercaptoethanol) and separated on 10% or 15% SDS polyacrylamide gels. After blocking in 3% skim milk powder, membranes were labeled with primary antibody (anti-LOC38715, 1.5 μg/ml, or anti-ERK1/2, 0.1 μg/ml; Sigma-Aldrich). Labeling was done with a secondary antibody to rabbit Ig conjugated with horseradish peroxidase (1:10,000) (Calbiochem) facilitating detection by chemiluminescence (Pierce).

Immunoprecipitation. Tissue samples (150–250 mg) were homogenized as described[27] and centrifuged at 500*g* to remove cell debris. We normalized the supernatants to soluble ERK1/2 and applied adjusted amounts of supernatant to protein G-sepharose beads (Sigma-Aldrich) conjugated with ARMS2 polyclonal antibodies. Beads were then washed six times in PBS and subsequently boiled in 1× Laemmli buffer. The suspension was subjected to protein blot analysis.

Immunohistochemistry. Retinal sections from human donor eyes were prepared for immunohistochemistry as described[17]. Sections were stained with the following primary antibodies: polyclonal antibody to ARMS2 (1:75), monoclonal antibody RS1-3R10 (1:250) specific to human retinoschisin[28], monoclonal rhodopsin-specific antibody Rho-1D4 (1:200), and mitochondrial marker monoclonal antibody MTCO2 (1:5,000). Subsequently, sections were incubated with Alexa conjugated secondary antibodies (1:1,000, Molecular Probes). Sections were counterstained with 4,6-diamidino-2-phenylindol (DAPI; Molecular Probes).

Accession codes. GenBank: *ARMS2* isoform 1, NM_001099667; *HTRA1*, NM_002775; genomic *ARMS2* indel variant reported in this manuscript (isoform 2), EU427539.

Note: Supplementary information is available on the Nature Genetics website.

ACKNOWLEDGMENTS

We are grateful to the individuals with AMD and the control subjects for their participation in this study; G. Huber for help with placental samples; P. Lichtner and T. Meitinger for SNP genotyping, R.S. Molday (Department of Biochemistry and Molecular Biology, University of British Columbia, Vancouver, Canada) for kindly sharing monoclonal antibodies RS1-3R10 and Rho-1D4, F.R. Rauscher (Institute of Human Genetics, University of Regensburg, Germany) for providing *ARMS2* cDNA clones of isoforms 1 and 2, and D. Wagner for technical assistance. This work was supported in part by grants to B.H.F.W. from the German Research Foundation (DFG), the Ruth and Milton Steinbach Foundation New York (B.H.F.W.) and the Alcon Research Institute.

AUTHOR CONTRIBUTIONS

L.G.F., T.L., A.J. and A.R. carried out all experimental studies. Specifically, L.G.F. participated in conception and design of the association study, was involved in all aspects of genotyping and data analysis and drafted the manuscript. T.L. made major contributions to the generation of ARMS2 antibodies and was responsible for all aspects of the protein work. A.J. carried out the immunohistochemistry studies. A.R. was involved in data acquisition and the characterization of *ARMS2* isoforms and carried out the RNA work. S.A.F. performed the statistical analyses and critically revised the manuscript. C.N.K. recruited the individuals with AMD and the controls and collected the peripheral blood samples. B.H.F.W. conceived of the study, participated in its design and coordination and finalized the manuscript. All authors read and approved the final text.

Published online at http://www.nature.com/naturegenetics/
Reprints and permissions information is available online at http://npg.nature.com/reprintsandpermissions/

1. Mitchell, P., Smith, W., Attebo, K. & Wang, J.J. Prevalence of age-related maculopathy in Australia. The Blue Mountains Eye Study. *Ophthalmology* **102**, 1450–1460 (1995).
2. Vingerling, J.R. *et al.* The prevalence of age-related maculopathy in the Rotterdam Study. *Ophthalmology* **102**, 205–210 (1995).
3. Seddon, J.M., Ajani, U.A. & Mitchell, B.D. Familial aggregation of age-related maculopathy. *Am. J. Ophthalmol.* **123**, 199–206 (1997).
4. Klein, R.J. *et al.* Complement factor H polymorphism in age-related macular degeneration. *Science* **308**, 385–389 (2005).
5. Edwards, A.O. *et al.* Complement factor H polymorphism and age-related macular degeneration. *Science* **308**, 421–424 (2005).
6. Haines, J.L. *et al.* Complement factor H variant increases the risk of age-related macular degeneration. *Science* **308**, 419–421 (2005).
7. Hageman, G.S. *et al.* A common haplotype in the complement regulatory gene factor H (HF1/CFH) predisposes individuals to age-related macular degeneration. *Proc. Natl. Acad. Sci. USA* **102**, 7227–7232 (2005).
8. Jakobsdottir, J. *et al.* Susceptibility genes for age-related maculopathy on chromosome 10q26. *Am. J. Hum. Genet.* **77**, 389–407 (2005).
9. Rivera, A. *et al.* Hypothetical LOC387715 is a second major susceptibility gene for age-related macular degeneration, contributing independently of complement factor H to disease risk. *Hum. Mol. Genet.* **14**, 3227–3236 (2005).
10. Dewan, A. *et al.* HTRA1 promoter polymorphism in wet age-related macular degeneration. *Science* **314**, 989–992 (2006).
11. Yang, Z. *et al.* A variant of the HTRA1 gene increases susceptibility to age-related macular degeneration. *Science* **314**, 992–993 (2006).
12. Kanda, A. *et al.* A variant of mitochondrial protein LOC387715/ARMS2, not HTRA1, is strongly associated with age-related macular degeneration. *Proc. Natl. Acad. Sci. USA* **104**, 16227–16232 (2007).
13. Grau, S. *et al.* The role of human HtrA1 in arthritic disease. *J. Biol. Chem.* **281**, 6124–6129 (2006).
14. Khabar, K.S. The AU-rich transcriptome: more than interferons and cytokines, and its role in disease. *J. Interferon Cytokine Res.* **25**, 1–10 (2005).
15. Barreau, C., Paillard, L. & Osborne, H.B. AU-rich elements and associated factors: are there unifying principles? *Nucleic Acids Res.* **33**, 7138–7150 (2005).
16. Garneau, N.L., Wilusz, J. & Wilusz, C.J. The highways and byways of mRNA decay. *Nat. Rev. Mol. Cell Biol.* **8**, 113–126 (2007).
17. Molday, L.L., Hicks, D., Sauer, C.G., Weber, B.H. & Molday, R.S. Expression of X-linked retinoschisis protein RS1 in photoreceptor and bipolar cells. *Invest. Ophthalmol. Vis. Sci.* **42**, 816–825 (2001).
18. Zeviani, M. & Carelli, V. Mitochondrial disorders. *Curr. Opin. Neurol.* **20**, 564–571 (2007).
19. Zarbin, M.A. Current concepts in the pathogenesis of age-related macular degeneration. *Arch. Ophthalmol.* **122**, 598–614 (2004).
20. Lin, M.T. & Beal, M.F. Mitochondrial dysfunction and oxidative stress in neurodegenerative diseases. *Nature* **443**, 787–795 (2006).
21. Gabriel, S.B. *et al.* The structure of haplotype blocks in the human genome. *Science* **296**, 2225–2229 (2002).
22. Barrett, J.C., Fry, B., Maller, J. & Daly, M.J. Haploview: analysis and visualization of LD and haplotype maps. *Bioinformatics* **21**, 263–265 (2005).
23. Dudbridge, F. Pedigree disequilibrium tests for multilocus haplotypes. *Genet. Epidemiol.* **25**, 115–121 (2003).
24. Dudbridge, F. UNPHASED user guide. Technical Report 5. (MRC Biostatistics Unit, Cambridge, 2006).
25. Fisher, S.A. *et al.* Case-control genetic association study of fibulin-6 (FBLN6 or HMCN1) variants in age-related macular degeneration (AMD). *Hum. Mutat.* **28**, 406–413 (2007).
26. Geysen, H.M., Rodda, S.J., Mason, T.J., Tribbick, G. & Schoofs, P.G. Strategies for epitope analysis using peptide synthesis. *J. Immunol. Methods* **102**, 259–274 (1987).
27. Fernandez-Vizarra, E., Lopez-Perez, M.J. & Enriquez, J.A. Isolation of biogenetically competent mitochondria from mammalian tissues and cultured cells. *Methods* **26**, 292–297 (2002).
28. Wu, W.W. & Molday, R.S. Defective discoidin domain structure, subunit assembly, and endoplasmic reticulum processing of retinoschisin are primary mechanisms responsible for X-linked retinoschisis. *J. Biol. Chem.* **278**, 28139–28146 (2003).